

Nitrogen and Oxygen Nuclear Quadrupole and Nuclear Magnetic Resonance Spectroscopic Study of N—O Bonding in Pyridine 1-Oxides*

Peter M. Woyciesjes, Nathan Janes, S. Ganapathy, Yukio Hiyama, Theodore L. Brown† and Eric Oldfield†

School of Chemical Sciences, University of Illinois at Urbana-Champaign, 505 South Mathews Avenue, Urbana, Illinois 61801, USA

¹⁴N nuclear quadrupole resonance (NQR) spectra of the NO functional group in a series of 4-substituted pyridine 1-oxides (R=H, CH₃, C₆H₅, OCH₃, OCH₂C₆H₅, Cl, CN, NO₂) and the natural abundance ¹⁷O NQR and nuclear magnetic resonance (NMR) solution spectra of a number of selected systems were obtained. The orientations of the principal axes of the ¹⁴N electric field gradient tensor (efg) in the NO group were determined using a Townes–Dailey treatment of the NQR results, combined with a ¹³C cross-polarization magic-angle sample-spinning NMR line shape analysis of carbons bonded directly to nitrogen. The major principal axis (Z) is coincident with the N—O bond. The orientation of the principal (Z) axis of the ¹⁷O efg tensor also lies along the N—O bond, as determined by Townes–Dailey analysis. The N—O π -bond orders show considerable sensitivity to the nature of the *para*-substituent, ranging from 0.17 to 0.31. ¹⁷O and ¹⁵N NMR chemical shifts parallel these changes in π -bond order.

Aromatic heterocyclic *N*-oxides have elicited considerable chemical, pharmacological and theoretical interest.^{1–4} Fundamental to their chemistry is the dual π -electron donor-acceptor role of the NO moiety, through resonance with the aromatic system.⁵ Thus, the N—O π bond is especially sensitive to the nature of ring substituents. Qualitative information concerning the N—O bond character has been obtained using various spectroscopic techniques, including UV,⁶ IR,⁷ photoelectron,⁸ dipole moments,⁹ gas-phase electron diffraction,¹⁰ microwave,¹¹ x-ray diffraction^{12–16} and carbon/nitrogen NMR methods.^{17,18} We believe, however, that there remains a need for a more quantitative probe of the electronic environment of the NO moiety, and that nuclear quadrupole resonance (NQR) spectroscopy of the ¹⁴N and ¹⁷O nuclei can provide such information, since the quadrupole resonance spectrum is determined by the electric field gradient (efg) tensor at the quadrupolar nucleus, and the field gradient, in turn, is determined mainly by the valence shell p-orbital populations of the atom containing the nucleus in question.

The quadrupole coupling constants of light elements, such as ¹⁴N and ¹⁷O, are conveniently interpreted in terms of the Townes–Dailey model,¹⁹ whereby the efg is ascribed to imbalances in the 2p orbital populations of the atom containing the quadrupolar nucleus. Application of the Townes–Dailey model does, however, require assumption, or experimental determination, of the orientation of the principal axes of the efg tensor. Until recently, the determination of the efg tensor orientation required

tedious and often difficult measurements on single crystals. Recently, however, it has been shown that in favorable cases information concerning the efg tensor orientation, and the sign of the quadrupole coupling constant, can be obtained from solid-state ¹³C cross-polarization ‘magic-angle’ spinning (CP-MAS) NMR experiments.²⁰ Although such information is not very precise, it is very useful in cases of high molecular symmetry when only the correct labeling of the principal efg axes is required.

In this paper we report the ¹⁴N and natural abundance ¹⁷O NQR spectra for a series of 4-substituted pyridine 1-oxides. The quadrupole coupling constants and asymmetry parameters vary substantially with substituent character, and are interpreted in terms of changes in valence p-orbital populations of the N—O nitrogen and oxygen atoms by means of a Townes–Dailey analysis. The results are shown to yield π -bond orders which correlate well with experimental ¹⁷O and ¹⁵N NMR chemical shifts in solution.

EXPERIMENTAL

Nuclear quadrupole resonance spectroscopy

¹⁴N and ¹⁷O NQR spectra were obtained on polycrystalline samples, using adiabatic demagnetization in the laboratory frame (ADLF) double-resonance techniques.^{21–23} Spectra at 77 K were obtained on 2–5 g samples, using the spectrometer described previously.²¹ A new instrument of similar overall design, but with variable temperature capability (*ca* 20–300 K), reduced sample size requirement (0.1–1 g) and

* Research supported in part by the National Institutes of Health (grants GM-23395 and HL-19481) and by the National Science Foundation (grants DMR 77-23999 and PCM 81-17813).

† Authors to whom correspondence should be addressed.

provision for computer-controlled signal averaging, was used for higher temperature work. A full description of this system is given elsewhere.²² The quadrupolar (S) spin system irradiation channel in each spectrometer contains an automatic tuning circuit which operates from 20 kHz to 7 MHz, together with provision for 180° r.f. phase shifting.

Nuclear magnetic resonance spectroscopy

All ¹³C CP-MAS NMR experiments were performed at room temperature on a double resonance spectrometer employing a 3.52 T (37.8 MHz for ¹³C) superconducting solenoid (Nalorac Cryogenics, Concord, CA) equipped with a Nicolet (Madison, WI) 1280 computer system, and a 'home-built' magic-angle sample-spinning probe, which typically operates at a spinning frequency of 1–3 kHz. Cross-polarization was established through a matched Hartmann–Hahn condition at r.f. amplitudes of 4.8 mT for ¹³C and 1.2 mT for ¹H. A single contact of 0.5–1.0 ms was employed, together with a sample-dependent recycle time of 2–15 s. Phase alternation was used to reduce baseline and intensity artifacts. The magic angle was set using an internal standard of crystalline reagent-grade KBr, maximizing the intensity of the second ⁷⁹Br spinning side band with respect to the center band.²⁴

¹⁷O NMR spectra were obtained using a second 'home-built' instrument, consisting of an 11.7 T 2.0-in bore superconducting solenoid (Oxford Instruments, Osney Mead, UK), a Nicolet 1280 computer system, a variety of digital and r.f. electronics and a 'home-built' solenoid coil probe; 90° pulse widths were typically 10 μs and the sample volume was ca 0.7 ml.

Materials

Reagent-grade pyridine 1-oxide, 4-methylpyridine 1-oxide and 2-methylpyridine 1-oxide were obtained from Reilly Tar and Chemical (Indianapolis, IN). Reagent-grade 4-nitropyridine 1-oxide, 4-methoxy-pyridine 1-oxide, 4-cyanopyridine 1-oxide and 4-phenylpyridine 1-oxide were obtained from Aldrich Chemical Co. (Milwaukee, WI). The 4-chloro and 4-benzyloxy derivatives were prepared from the 4-nitro derivative following the method of Ochiai.²⁵ With the exception of the 4-chloro compounds, all the 4-substituted 1-oxides were purified by recrystallization from aqueous ethanol.²⁶ Pyridine 1-oxide and 4-chloropyridine 1-oxide were purified by repeated vacuum sublimation at 110 and 100 °C, respectively. Manipulation of these two very hygroscopic compounds was carried out in a dry-box. Acetonitrile was distilled over P₂O₅ prior to use.

RESULTS AND DISCUSSION

The ¹⁴N and ¹⁷O NQR data obtained for the pyridine 1-oxides are listed in Tables 1 and 2, respectively. The $I = 5/2$ ¹⁷O NQR transition frequencies were solved

Table 1. ¹⁴N quadrupole resonance frequency and efg parameters for 4-substituted pyridine 1-oxides

Substituent	ν_+ (kHz)	ν_- (kHz)	ν_0 (kHz)	e^2Qq_{zz}/h (MHz)	η
NO ₂	1043	629	413	1.115	0.741
CN	1087	662	425	1.166	0.730
H	1084	699	385	1.188	0.648
C ₆ H ₅	1104	929	175	1.355	0.258
CH ₃	1171	930	241	1.401	0.344
Cl	1150	976	174	1.417	0.245
OCH ₂ C ₆ H ₅	1178	1067	—	1.497	0.148
OCH ₃	1255	1142	—	1.598	0.142

Table 2. ¹⁷O quadrupole resonance frequency and efg parameters for the N—O functional group for a series of 4-substituted pyridine 1-oxides at 110 K^{a,b}

Substituent	$\nu_{\pm 3/2 \rightarrow \pm 5/2}$ (kHz)	$\nu_{\pm 1/2 \rightarrow \pm 3/2}$ (kHz)	e^2Qq_{zz}/h (MHz)	η
NO ₂	4130	2930	14.62	0.603
H	4410	2760	15.26	0.457
Cl	4578	2648	15.63	0.356
CH ₃	4594	2606	15.63	0.329
OCH ₂ C ₆ H ₅	4780	2645	16.20	0.292

^a NO₂ oxygens: $e^2Qq_{zz}/h = 13.24$ MHz, $\eta = 0.606$: $\nu_{\pm 3/2 \rightarrow \pm 5/2} = 2660$ kHz, $\nu_{\pm 1/2 \rightarrow \pm 3/2} = 3740$ kHz. $e^2Qq_{zz}/h = 12.89$ MHz, $\eta = 0.590$: $\nu_{\pm 3/2 \rightarrow \pm 5/2} = 2560$ kHz, $\nu_{\pm 1/2 \rightarrow \pm 3/2} = 3650$ kHz.

^b OCH₂C₆H₅ oxygen: $e^2Qq_{zz}/h = 9.85$ MHz, $\eta = 0.696$: $\nu_{\pm 3/2 \rightarrow \pm 5/2} = 2740$ kHz, $\nu_{\pm 1/2 \rightarrow \pm 3/2} = 2110$ kHz.

exactly as described elsewhere.²⁷ Only one site was observed for ¹⁴N and ¹⁷O NQR of the parent pyridine 1-oxide at 77 and 110 K, respectively, despite the room temperature x-ray structure, which indicates two sites.¹³ However, owing to the great imprecision of the x-ray data, we do not regard the two sites as necessarily distinct.

Analysis of the ¹⁴N NQR results

The electronic environment of nitrogen may be probed by NQR and interpreted in terms of the Townes–Dailey model when the orientation of the electric field gradient (efg) principal axes are known. The approximate C_{2v} symmetry of the 4-substituted pyridine 1-oxides restricts the assignment of axis systems to six cases, using the convention $|q_{zz}| \geq |q_{yy}| \geq |q_{xx}|$. One efg axis lies along the N—O bond, bisecting the C—N—C angle, while another is normal to the molecular plane and a third is perpendicular to the N—O bond in the molecular plane (Fig. 1A). Each of the six assignments may correspond to either a positive or a negative quadrupole coupling constant, yielding a total of twelve cases. The proper assignment can be made as follows: (a) CP-MAS ¹³C NMR reduces the possibilities to four by assigning q_{zz} in the molecular frame; (b) a Townes–Dailey analysis as a function of substituent character for the four remaining choices narrows the possibilities to two; and (c) the remaining pair of assignments are distinguished on the basis of reasonable N—O σ -bond populations obtained with the Townes–Dailey model and applied to pyridine 1-oxide and 4-cyanopyridine 1-oxide.

¹³C CP-MAS NMR results. Magic-angle spinning does not completely remove the dipolar coupling between

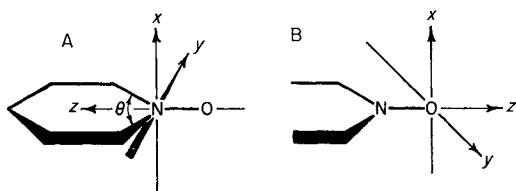


Figure 1. ¹⁴N (A) and ¹⁷O (B) molecular axis systems used in the Townes–Dailey model.

¹⁴N and ¹³C when carbon is directly bonded to nitrogen,²⁰ resulting in a splitting or broadening of the ¹³C resonances. This effect is due to perturbation of the ¹³C–¹⁴N dipolar interaction because of mixing of the ¹⁴N Zeeman states, and becomes significant in systems where the Zeeman and quadrupole energy terms are of the same order of magnitude. The line shape is sensitive to both the sign and magnitude of the ¹⁴N efg tensor components, the angle between the principal axes of the dipolar and quadrupolar tensors and the strength of the static field and the spinning frequency.

The resonances of carbon bonded to nitrogen can be simulated for the six possible axis systems and com-

pared with the experimental line shape, as shown in Fig. 2. For simplicity, the sign of the quadrupole coupling constant is taken as positive—negative coupling constants result in respective mirror image spectra.²⁰ Simulations and experimental line shapes are shown for C-6 of 2-methylpyridine 1-oxide. Assignments were made from ¹³C solution data¹⁷ and assigned to the CP-MAS spectra as shown in Fig. 3.

The carbon resonances of interest in each case are quite symmetric. The 2-methyl substituent was chosen because the C-2 and C-6 resonances were well separated, and because the nitrogen electronic environment should be similar to pyridine 1-oxide. The infrared N–O stretch frequency of 2-methylpyridine 1-oxide is very similar to that of the parent compound, suggesting little perturbation due to the steric effects observed for certain *ortho*-substituted heterocyclic *N*-oxides.²⁸

In order to preclude the possibility that the symmetric C-2, C-6 line shapes were due to an effective decoupling of the ¹⁴N spins caused by rapid ¹⁴N spin-lattice relaxation,²⁹ a spectrum of 2-methylpyridine 1-oxide was obtained at 15.1 MHz (1.4 T). The peaks for C-2 and C-6 are broader and relatively weak

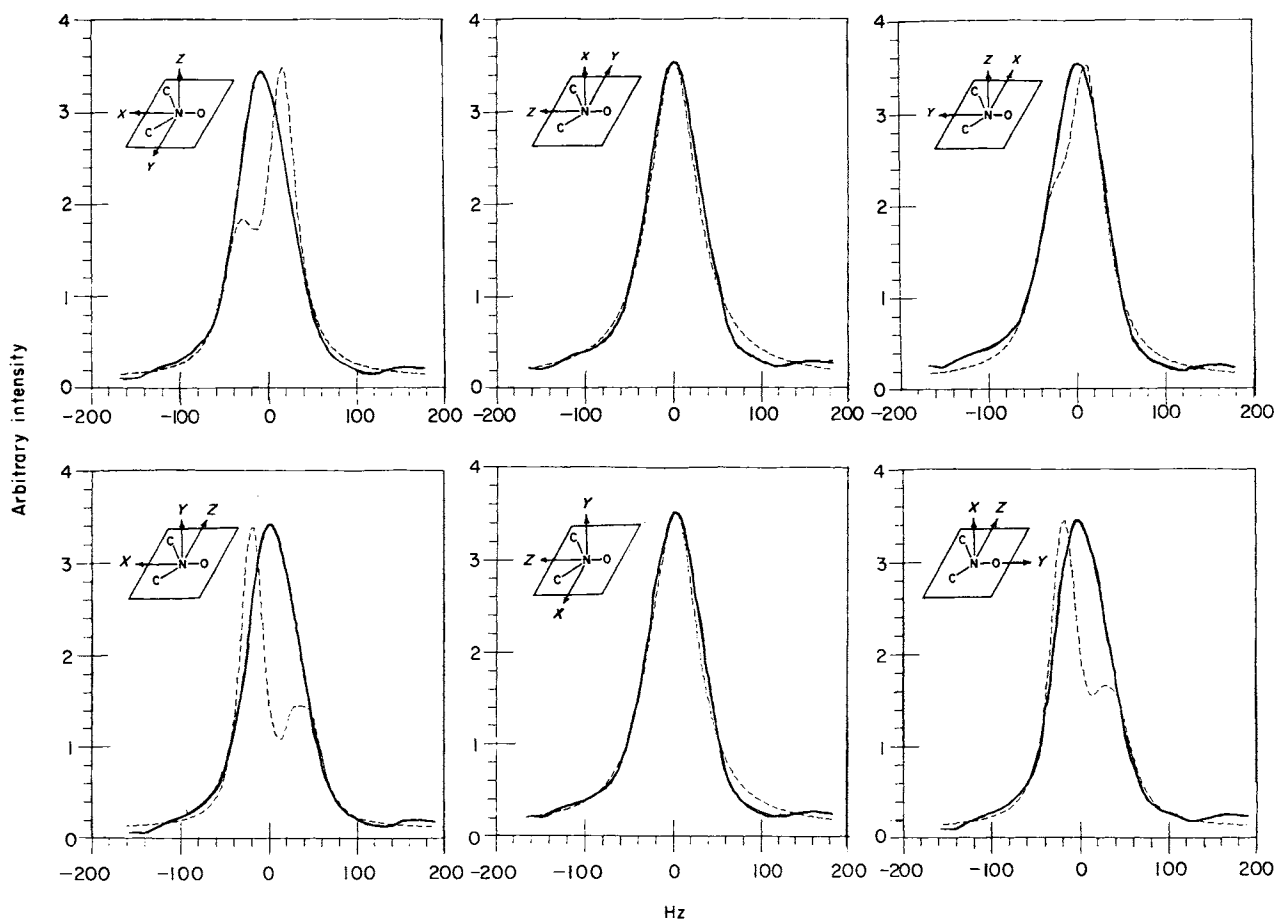


Figure 2. Comparison of the experimental (solid line) and theoretical (dashed line) ¹³C line shapes of the 2-methylpyridine 1-oxide C-6 carbon (bonded to nitrogen), assuming the principal efg axis system for ¹⁴N as shown. The simulations presented correspond to a positive quadrupole coupling constant. Those cases corresponding to a negative quadrupole coupling constant are not shown, but are represented by the respective mirror images of the simulations. The theoretical fit to the experimental line shape is best for the principal efg Z axis along the N–O bond. $e^2Qq/h = 1.299$ MHz, $\eta = 0.238$, $\nu_+ = 1052$ kHz, $\nu_- = 897$ kHz, $\gamma_C\gamma_N h/4\pi^2 r_{CN}^3 = 0.830$ kHz, $\gamma_N \hbar H_0 = 10.86$ MHz. Lorentzian broadening sufficient to match the full width at quarter height varied from 15 to 35 Hz.

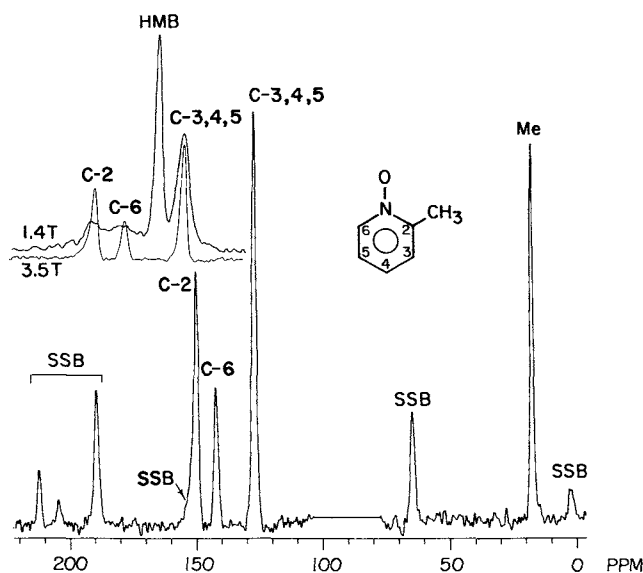


Figure 3. 3.5 T CP-MAS ^{13}C spectrum of 2-methylpyridine 1-oxide. The Delrin spinner peak has been truncated. Inset: aromatic region of 2-methylpyridine 1-oxide at two different field strengths. The broadening of the carbon resonances bonded directly to nitrogen at 1.4 T indicates that the symmetric line shapes observed are a consequence of a particular orientation of the efg tensor and not a result of rapid ^{14}N relaxation. (C-2 = 149.3 ppm; C-6 = 141.5 ppm; C-3,4,5 = 126.3 ppm; CH_3 = 17.1 ppm from TMS.) SSB, spinning side band; HMB, hexamethylbenzene internal standard.

compared with the high-field spectrum, as shown in Fig. 3. We conclude that the symmetric line shapes are a consequence of the orientation of q_{zz} (Fig. 1A) along the C_2 symmetry axis. On this basis, only two axis systems are realistic, and the sign of the quadrupole coupling constant is undetermined. As a result, four possibilities remain.

Townes–Dailey analysis of substituent effects. The 4-substituted pyridine 1-oxides studied by diffraction techniques are planar molecules,^{12–15} with the nitrogen valence p orbital normal to the plane. The nitrogen 2p orbital participates in π bonding, both to the ring and to oxygen. The principal values of the efg tensor, as oriented in Fig. 1A, are related to the orbital populations σ_{NC} , σ_{NO} and p_π as follows:

$$q_{XX}/q_{210} = p_\pi + (1/2)(s-1)\sigma_{\text{NO}} - (1/2)(1+s)\sigma_{\text{NC}} \quad (1)$$

$$q_{YY}/q_{210} = (-1/2)p_\pi + (1/2)(s-1)\sigma_{\text{NO}} + (1/2)(2-s)\sigma_{\text{NC}} \quad (2)$$

$$q_{ZZ}/q_{210} = (-1/2)p_\pi + (1-s)\sigma_{\text{NO}} + (1/2)(2s-1)\sigma_{\text{NC}} \quad (3)$$

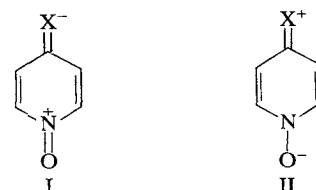
$$s = \cot^2(\theta/2) \quad (4)$$

where s is the hybrid s character of the sp^2 orbitals determined by the CNC bond angle θ , and q_{210} is the field gradient at the nitrogen nucleus generated by a single $2p_z$ electron, where $e^2q_{210}Q/h = -9.1$ MHz.²² These equations can be rewritten in terms of the quadrupole coupling constant and asymmetry parameter (η) for the orientation in Fig. 1A,

$$p_\pi - \sigma_{\text{NC}} = \pm(2/3)\eta(e^2Qq_{zz}/e^2Qq_{210}) \quad (5)$$

$$\sigma_{\text{NO}} - \sigma_{\text{NC}} = (1/1-s)[1 \pm (\eta/3)](e^2Qq_{zz}/e^2Qq_{210}) \quad (6)$$

where the ambiguity in sign is due to uncertainty as to the relative magnitudes of q_{XX} and q_{YY} . The Townes–Dailey treatment, applied to the remaining four possible combinations, provides occupancy values of the nitrogen π orbital, p_π , and the nitrogen σ orbital employed in bonding to oxygen, σ_{NO} , if a value is chosen for both the nitrogen orbital occupancy employed in bonding to carbon, σ_{NC} , and the hybrid s character, s . Noting that, in general, the σ orbitals are less sensitive to substituent changes than the π orbitals, we adopt $\sigma_{\text{NC}} = 1.3$, as found for pyridine.³⁰ Accurate determination of the hybrid s character, s , relies on crystal structure data. A correlation between increasing N—O π -bond order and decreasing CNC angle, θ , had been proposed,¹⁶ but subsequent investigations cast doubt on any regular trend.^{10,12} Since the orbital populations are very sensitive to the choice of θ (or equivalently the hybrid s character, s), we choose to use Eqn (5) and correlate the p_π occupancy with the nature of the *para*-substituent, thereby eliminating any uncertainty resulting from changing the s character of hybridization. In particular, we are interested in the resonance contribution of the substituent, as opposed to the inductive contribution. These contributions are represented by the Taft parameters σ_R and σ_I , respectively. The σ_R values are derived from $\sigma(\text{PyNO})$ constants (obtained from the acid dissociation constants of substituted pyridine 1-oxides³¹) using Taft's³² σ_I values where $\sigma_R(\text{PyNO}) = \sigma(\text{PyNO}) - \sigma_I$. Electron-withdrawing substituents via resonance are expected to decrease the nitrogen p_π orbital population so that canonical form I becomes important. Electron-donating substituents via resonance are expected to exhibit the opposite effect, so that canonical form II becomes important.



The nitrogen p_π orbital populations are listed in Table 3 for various 4-substituted pyridine 1-oxides in the four remaining possible cases where the efg z -axis lies along the N—O bond.

Table 3. ^{14}N p_π occupancy for a series of 4-substituted pyridine 1-oxides^a

Substituent	$ zz \geq yy \geq xx ^b$		$ zz \geq xx \geq yy ^b$		$\sigma_R(\text{PyNO})^c$
	$e^2Qq_{zz} > 0$	$e^2Qq_{zz} < 0$	$e^2Qq_{zz} > 0$	$e^2Qq_{zz} < 0$	
NO_2	1.240	1.360	1.360	1.240	+0.56
CN	1.238	1.362	1.362	1.238	+0.35
H	1.244	1.356	1.356	1.244	0.00
C_6H_5	1.274	1.326	1.326	1.274	-0.09 ^d
CH_3	1.265	1.335	1.335	1.265	-0.19
Cl	1.275	1.325	1.325	1.275	-0.26
OCH_3	1.283	1.317	1.317	1.283	-0.83
$\text{OCH}_2\text{C}_6\text{H}_5$	1.284	1.316	1.316	1.284	—

^a Shown are the four possible combinations of sign and axis system when the principal Z axis is fixed along the N—O bond, assuming $\sigma_{\text{CN}} = 1.3$, $e^2Qq_{210}/h = -9.1$ MHz.

^b Referenced to the molecular axis system shown in Fig. 1A.

^c Calculated as described in the text.

^d σ_R calculated from the benzoic acid σ .

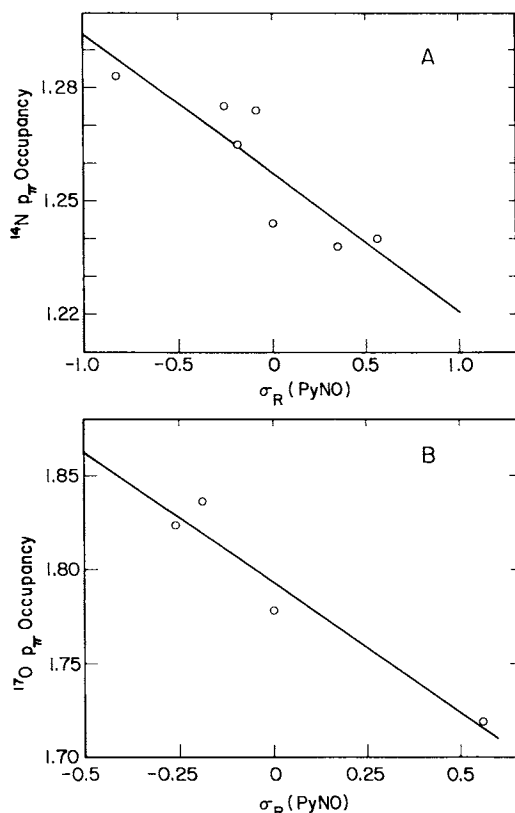


Figure 4. Correlation between ¹⁴N (A) and ¹⁷O (B) p_π occupancies of the 4-substituted pyridine 1-oxides as a function of Taft parameters.

Clearly the first and fourth cases follow the expected trend. Both cases contain identical p_π occupancies.

The correlation between p_π occupancy and substituent character, $\sigma_R(\text{PyNO})$, (correlation coefficient 0.87, $n = 7$), as shown in Fig. 4A is reasonably good, and compares favorably with a similar correlation found by others for the 4-substituted pyridines (correlation coefficient 0.75, $n = 5$).³³

Townes–Dailey analysis of σ_{NO} occupancy. The two possibilities that remain contain identical p_π occupancies, but very different σ_{NO} occupancies. The Townes–Dailey model can be applied to the parent pyridine 1-oxide and the 4-cyano derivative, since crystal structures have been reported,^{13,16} so that a reasonable estimate of s hybridization can be made. The Townes–Dailey orbital occupancies for the 4-cyano and parent pyridine 1-oxide are listed in Table 4 based on $\theta = 119.4^\circ$ and 122° , respectively. Since oxygen is more electronegative than nitrogen, a σ_{NO} population of approximately 1 or slightly less is expected, while

Table 4. ¹⁴N Townes–Dailey treatment of σ_{NO} populations^a

$ zz \geq yy \geq xx $, ^b $e^2Qq_{zz} > 0$		$ zz \geq xx \geq yy $, ^b $e^2Qq_{zz} < 0$	
$\sigma_{\text{NO}}(\text{CN})$	$\sigma_{\text{NO}}(\text{H})$	$\sigma_{\text{NO}}(\text{CN})$	$\sigma_{\text{NO}}(\text{H})$
1.058	1.071	1.447	1.448

^a $\theta_{\text{CN}} = 119.4^\circ$; $\theta_{\text{H}} = 122^\circ$.

^b Referenced to the molecular axis system shown in Fig. 1A.

occupancies similar to σ_{NC} (1.3) are clearly unreasonable. The first case listed in Table 4 thus appears to correspond to the correct assignment of efg axes on ¹⁴N. We can conclude that the principal axes, X, Y, and Z, are collinear with the molecular axes, x , y and z , shown in Fig. 1A, and that the quadrupole coupling constant is positive. The good correlation between $\sigma_{\text{R}}(\text{PyNO})$ and p_π suggests that the principal axis system has the same orientation for all the substituents examined.

Analysis of the ¹⁷O NQR results

In previous work the Townes–Dailey analysis has been applied to ¹⁷O bonded to nitrogen, sulfur, phosphorus³⁴ and carbon.³⁵ The ¹⁷O molecular orbitals can be described in terms of the molecular axis system of Fig. 1B. An sp hybrid set lies along the N–O bond. The N–O bonding orbital has a population p_σ . There is also a p orbital, of population p_π , which can participate in π bonding along the molecular x axis, and a lone-pair p orbital of population 2, unable to conjugate with the ring, along y . Using this molecular orbital framework the efg tensor axes are as follows:

$$q_{zz}/q_{210} = -1 - (p_\pi/2) + p_\sigma^0$$

$$q_{yy}/q_{210} = 2 - (p_\pi/2) - (p_\sigma^0/2)$$

$$q_{xx}/q_{210} = -1 + p_\pi - (p_\sigma^0/2)$$

where $e^2q_{210}Q/h = 20.9 \text{ MHz}$ and $p_\sigma^0 = p_\sigma(1-s) + 2s$ includes the s character of hybridization, s . As was the case for nitrogen, there are six possible assignments of the efg tensor principal axes (X, Y and Z) relative to the molecular axis system (x , y , z), in addition to the two possible signs of the quadrupole coupling constant. The twelve possible combinations and their respective orbital populations are listed in Table 5 for the parent pyridine 1-oxide.

Table 5. Analysis of the ¹⁷O NQR data of the N–O group in pyridine 1-oxide for all possible orientations of the principal X, Y and Z axes relative to the molecular axis system x , y and z ^{a,b,c}

Case	Relative magnitude of efg tensor components	Sign of e^2Qq_{zz}/h	p_π	p_σ^0
1	$ zz \geq yy \geq xx $	+	2.222	2.841
2	$ zz \geq xx \geq yy $	+	1.777	2.619
3	$ yy \geq zz \geq xx $	+	1.381	1.159
4	$ yy \geq xx \geq zz $	+	1.158	1.381
5	$ xx \geq zz \geq yy $	+	2.619	1.778
6	$ xx \geq yy \geq xx $	+	2.841	2.222
7	$ zz \geq yy \geq xx $	-	1.778	1.157
8	$ zz \geq xx \geq yy $	-	2.222	1.381
9	$ yy \geq zz \geq xx $	-	2.619	2.841
10	$ yy \geq xx \geq zz $	-	2.841	2.619
11	$ xx \geq zz \geq yy $	-	1.381	2.222
12	$ xx \geq yy \geq zz $	-	1.159	1.778

^a $e^2Qq_{210}/h = 20.9 \text{ MHz}$.

^b $e^2Qq_{zz}/h = 15.26 \text{ MHz}$, $\eta = 0.457$ for pyridine 1-oxide.

^c Referenced to the molecular axis system shown in Fig. 1B.

The feasibility of the assignments can be deduced from physically reasonable values for p_π and p_σ^0 . Neither value should exceed the full orbital population of 2. The N—O bond in pyridine 1-oxide should not be far removed from homopolar character; consequently, p_σ^0 is approximately 1. The value for p_π should be less than 2, depending on the extent of π back-bonding, which is not considered large for the parent compound. Clearly, only case 7 in Table 5 fits these criteria. That is, e^2Qq_{ZZ} is negative (eq_{ZZ} is positive since eQ is negative), the principal Z axis is collinear with the N—O bond, and the principal Y axis lies in the molecular plane.

In a previous study of various systems with N—O bonds,³⁴ it was reported that when the p_π occupancy is reduced to about 1.65 there is a change in the axis system and sign of the quadrupole coupling constant. This does not seem to be the case for the 4-substituted pyridine 1-oxides examined here. The principal axis system for the parent pyridine 1-oxide should apply equally well to the 4-substituted derivatives listed in Table 2. This view is reinforced by the very good correlation between ^{17}O p_π orbital occupancy and $\sigma_R(\text{PyNO})$ as shown in Fig. 4B (correlation coefficient 0.97, $n = 4$).

Both ^{17}O and ^{14}N exhibit a parallel reduction of the p_π orbital populations as the *para*-substituent becomes increasingly electron-withdrawing through resonance. Since eq_{ZZ} for both nuclei lies along the N—O bond and is positive, the quadrupole coupling constant decreases and the asymmetry parameter increases as the p_π orbital occupancy drops, and the N—O π -bond order grows larger.

π Bond order and chemical shifts

Both the ^{14}N and ^{17}O NQR results reflect the effect of ring substituents on the charge distribution in the N—O bond. The ^{17}O results are particularly interesting because the ^{17}O p_π population is directly related to the N—O π -bond order. A qualitative relationship expressing the N—O π -bond order in terms of the ^{17}O p_π populations has performed well in other N—O bonded systems.³⁴

$$p_\pi = 1.1x + 2(1 - x)$$

where x is the partial π -bond order. Results for p_π occupancy, π -bond order and formal charge are given in Table 6 for the ^{17}O nucleus. The π -bond order

Table 6. Summary of Townes–Dailey analysis of ^{17}O NQR and NMR chemical shift results for a series of 4-substituted pyridine 1-oxides

Substituent	p_π	p_σ^0 (0% s)	p_σ (10% s)	p_σ (20% s)	π bond order	Q^a	$\sigma_R(\text{PyNO})$	NMR shift ^b
$\text{OCH}_2\text{C}_6\text{H}_5$	1.849	1.149	1.054	0.936	0.168	-0.78	—	—
CH_3	1.836	1.170	1.078	0.963	0.182	-0.80	-0.19	330
Cl	1.823	1.163	1.070	0.954	0.197	-0.78	-0.26	348
H	1.778	1.159	1.066	0.949	0.247	-0.73	0.00	345
NO_2	1.719	1.160	1.067	0.950	0.312	-0.67	+0.56	412

^a $Q = 2 - p_\pi - p_\sigma$. Formal charge on oxygen assuming 20% s character (Ref. 34).

^b 0.33M in CH_3CN : δ (ppm) from external H_2O . Accuracy is ± 1 ppm.

exhibits the expected correlation with N—O infrared stretch frequencies⁷ (correlation coefficient 0.904, $n = 5$).

The NMR chemical shifts are very sensitive to the electronic environment of a given nucleus. Previous workers²⁸ have established a correlation between ^{15}N NMR chemical shifts in solution with N—O infrared stretch frequencies of heterocyclic *N*-oxides.

The nitrogen and oxygen chemical shift range is determined predominantly by the local paramagnetic term in the Karplus–Pople formalism:³⁶

$$\sigma_{\text{para}} = \frac{-e^2\hbar^2\langle r^{-3} \rangle_{2p}}{2m^2c^2(\Delta E)} \left[Q_{AA} + \sum_{B \neq A} (Q_{AB}) \right]$$

The paramagnetic contribution to the chemical shift of atom A bonded to atoms B is described in terms of the radial distribution of the p electrons, the average excitation energy ΔE and the ground-state charge density and bond order matrix, Q . The last term concerns only orbitals with non-zero angular momentum and represents the imbalance of orbital populations around nucleus A from a spherical electronic distribution. Similarly, the Townes–Dailey treatment is based on the imbalance of p orbital populations. Both treatments depend on the p-electron radial term $\langle r^{-3} \rangle$, which in the Townes–Dailey analysis is assumed to be constant and expressed as eq_{210} , the field gradient of a $2p_z$ electron at the nucleus.

We consider it instructive to correlate ^{15}N (or equivalently ^{14}N) and ^{17}O chemical shifts with the results of the Townes–Dailey analysis (bond order, charge density and p_π population) in the light of similar correlations based on the Karplus–Pople model.

^{14}N chemical shifts of the N—O moiety of azine *N*-oxides have been correlated with the SCF–PPP–MO π -charge density at the oxide nitrogen.³⁷ The PPP π -charge density reflects changes in the total charge density on nitrogen, since the term not only reflects the nitrogen p_π population, but also contributions from σ -bond polarizations.³⁸ Calculations applied to azine *N*-oxides using the INDO/S method exhibit good correlations of ^{14}N chemical shifts and the product $\langle r^{-3} \rangle \sum Q_{AB}$, a weighted measure of charge density.³⁹ The variation of ^{17}O chemical shift with π -bond order observed for metal–oxygen systems⁴⁰ stems predominantly from variations in the $\sum_{A \neq B} Q_{AB}$ term.

Our results show a good correlation of increasing N—O bond order (N—O mobile bond order in the Pople formalism) with increasing ^{15}N shielding¹⁷ (correlation coefficient 0.987, $n = 4$), whereas the correlation between p_π occupancy and ^{15}N shielding is somewhat less convincing (correlation coefficient 0.894, $n = 4$).

The ^{17}O chemical shifts appear to vary with N—O bond order as well as formal charge density (Table 6). The oxygen is deshielded as the bond order increases and as the charge density correspondingly decreases (correlation coefficients 0.917 and 0.908, respectively, $n = 4$).

These results suggest that the nitrogen and oxygen chemical shifts in the 4-substituted pyridine 1-oxides are a measure of N—O π -bond order, although more results are needed to quantify this relationship.

Further, the results suggest that the average energy approximation used for calculation of the local paramagnetic shift is valid in these compounds.

The N—O π -bond order, long believed to dominate the chemistry of the heterocyclic N-oxides, is very sensitive to *para*-substituent changes. We have found N—O π bonds with π -bond character ranging from 17 to 31%, indicating a substantial ability of the N—O

moiety to donate or withdraw charge density from the aromatic system.

Acknowledgement

We thank Dr Dennis A. Torchia of the National Institutes of Health for the use of the 1.4 T CP-MAS NMR spectrometer.

REFERENCES

1. A. R. Katritzky and J. M. Lagowski, *Chemistry of the Heterocyclic N-Oxides*. Academic Press, New York (1971).
2. E. Ochiai, *Aromatic Amine Oxides*. Elsevier, New York (1967).
3. N. M. Karayannis, L. L. Pytlewski and C. M. Mikulski, *Coord. Chem. Rev.* **11**, 93 (1973).
4. T.-K. Ha, *Theor. Chim. Acta* **43**, 337 (1977).
5. A. R. Katritzky, E. W. Randall and L. E. Sutton, *J. Chem. Soc.* 1769 (1957); A. R. Katritzky, A. M. Monro and J. A. T. Beard, *J. Chem. Soc.* 3721 (1958); A. R. Katritzky, *Recl. Trav. Chem. Pays-Bas* **78**, 995 (1959).
6. T. Kubota and H. Miyazaki, *Chem. Pharm. Bull.* **9**, 948 (1961).
7. H. Shindo, *Chem. Pharm. Bull.* **6**, 117 (1958).
8. J. P. Maier, J.-F. Muller and T. Kubota, *Helv. Chim. Acta* **58**, 1634 (1975).
9. E. P. Linton, *J. Am. Chem. Soc.* **62**, 1945 (1940).
10. J. F. Chiang and J. J. Song, *J. Mol. Struct.* **96**, 151 (1982).
11. O. Snerling, C. J. Nielsen, L. Nygaard, E. J. Pedersen and G. O. Sørensen, *J. Mol. Struct.* **27**, 205 (1975).
12. Y. Wang, R. H. Blessing, F. K. Ross and P. Coppens, *Acta Crystallogr., Sect. B* **32**, 572 (1976).
13. D. Üklü, B. P. Huddle, and J. C. Morrow, *Acta Crystallogr., Sect. B* **27**, 432 (1971).
14. G. Tsoucaris, *Acta Crystallogr.* **14**, 914 (1961).
15. E. L. Eichorn, *Acta Crystallogr.* **9**, 787 (1956).
16. K. I. Hardcastle, M. J. Laing, T. J. McGauley and C. F. Lehner, *J. Cryst. Mol. Struct.* **4**, 305 (1974).
17. I. Yavari and J. D. Roberts, *Org. Magn. Reson.* **12**, 87 (1979).
18. H. Günther and A. Gronenborn, *Heterocycles* **11**, 337 (1978).
19. C. H. Townes and B. P. Dailey, *J. Chem. Phys.* **17**, 782 (1949).
20. A. Naito, S. Ganapathy and C. A. McDowell, *J. Magn. Reson.* **48**, 367 (1982); A. Naito, S. Ganapathy and C. A. McDowell, *J. Chem. Phys.* **74**, 5393 (1981); J. G. Hexem, M. H. Frey and S. J. Opella, *J. Chem. Phys.* **77**, 3847 (1982), and references cited therein.
21. Y.-N. Hsieh, P. S. Ireland and T. L. Brown, *J. Magn. Reson.* **21**, 445 (1976).
22. D. A. D'Avignon, PhD Thesis, University of Illinois (1981); L. G. Butler, PhD Thesis, University of Illinois (1981).
23. R. E. Slusher and E. L. Hahn, *Phys. Rev.* **166**, 332 (1968).
24. J. S. Frye and G. E. Maciel, *J. Magn. Reson.* **48**, 125 (1982).
25. E. Ochiai, *J. Org. Chem.* **18**, 534 (1953).
26. D. W. Herlocker, R. S. Drago and V. I. Meek, *Inorg. Chem.* **5**, 2009 (1966).
27. R. B. Creel, H. R. Brooker and R. G. Barnes, *J. Magn. Reson.* **41**, 146 (1980).
28. W. W. Paudler and M. V. Jovanovic, *Heterocycles* **19**, 93 (1982).
29. G. E. Balimann, C. J. Groombridge, R. K. Harris, K. J. Packer, B. J. Say and S. F. Tanner, *Phil. Trans. R. Soc. London, Ser. A* **299**, 643 (1981).
30. G. V. Rubenacker and T. L. Brown, *Inorg. Chem.* **19**, 392 (1980).
31. J. H. Nelson, R. G. Garvey and R. O. Ragsdale, *J. Heterocycl. Chem.* **4**, 591 (1967).
32. R. W. Taft, Jr, in *Steric Effects in Organic Chemistry*, edited by M. S. Newman, Chapt. 13 Wiley, New York (1956).
33. E. A. C. Lucken, *Nuclear Quadrupole Coupling Constants*. Academic Press New York (1969).
34. C. P. Cheng and T. L. Brown, *J. Am. Chem. Soc.* **102**, 6418 (1980); Y. Hiyama and T. L. Brown, *J. Phys. Chem.* **85**, 1698 (1981); T. L. Brown and C. P. Cheng, *Symp. Faraday Soc.* **13**, 75 (1979).
35. C. P. Cheng and T. L. Brown, *J. Am. Chem. Soc.* **101**, 2327 (1979).
36. M. Karplus and J. A. Pople, *J. Chem. Phys.* **38**, 2803 (1963).
37. L. Stefaniak, *Spectrochim. Acta, Part A* **32**, 345 (1976).
38. M. Witanowski, L. Stefaniak, H. Januszewski and G. A. Webb, *J. Magn. Reson.* **16**, 69 (1974).
39. M. Witanowski, L. Stefaniak, B. Kamieński and G. A. Webb, *Org. Magn. Reson.* **14**, 305 (1980).
40. R. G. Kidd, *Can. J. Chem.* **45**, 605 (1967).

Received 20 April 1984; accepted (revised) 31 August 1984